

Design and Fabrication of a Spiral Electrode Triboelectric Nanogenerator and Application as Zero Power dynamic Sensor

M.A. Heydari

Ph.D. Candidate
Department of Electronics Engineering,
University of Sistan and Baluchestan,
Zahedan,
Iran

T. Fanaei Sheikholeslami

Associate Professor
Department of Mechanical and
Mechatronics Engineering, University of
Sistan and Baluchestan,
Zahedan,
Iran

A. Behzadmehr

Professor
Department of Mechanical and
Mechatronics Engineering, University of
Sistan and Baluchestan,
Zahedan,
Iran

Harvesting energy from environmental motions is an efficient method to prepare permanent power supplies for intelligent wireless systems. In this paper, a single spiral electrode triboelectric nanogenerator (TENG) is fabricated and investigated for energy harvesting from multi-directional sliding motions. The device is intended to be also used as a self-powered dynamic velocity sensor. In the first step, four samples are fabricated and characterized by applying 2 Hz sliding motions. The results show an increase in the output power from 1.53 to 20.72 nW, for a device with 4 to 20 turns. To compare the results, the effect of increasing the output power using a parallel array is also studied. In the next step, applications of the device as velocity and position sensors are investigated. A linear dependence between the input and output of the sensor is noticed for the device with 8, and 16 spiral turns. Finally, a circuit modeling for the device is presented, and a trend is suggested for the virtual capacitive behavior of the single electrode TENG.

Keywords: Energy harvesting, Triboelectric, Sliding motions, Spiral electrode, dynamic zero-power sensor

1. INTRODUCTION

Using clean and renewable energies is important due to the high growth of energy consumption worldwide and the environmental issues. It also has undeniable importance for self-biasing wireless systems. The new era relies heavily on technology, where the unavailability and limitations of stationary power supplies lead to the simultaneous need for renewable and portable resources. To address such requirements, the researchers highly consider harvesting the wasted environmental vibrations and converting it into electrical energy [1-2]. One of the simplest ideas for harvesting environmental energies is to employ the interesting properties of materials, such as piezoelectricity, thermoelectricity, triboelectricity, etc. In recent studies, hard or flexible triboelectric nanogenerators (TENGs) have been used to do such work based on the triboelectric properties of the materials [3-5]. Various types of vertical and sliding TENG devices have been fabricated, and their performances have been studied [3]. The reported works also contain the basic theory of TENGs and modeling of the device's performance [6]. Among them, sliding in-plane TENGs grab the attention of researchers more than other types of TENGs, due to their vast application in harvesting energy from all friction-based environmental movements and wearable, self-powered, active human motions [7]. By applying a repeatable sliding motion, alternating output current and voltage

will be produced. The motion of a sliding TENG can be rotational in a cylinder form with the possibility of using the device in hybrid generators [8-10]. The single-electrode TENG is also incorporated with the grating electrodes connected to a dielectric movable part [11-14]. As found in recent studies, in most single-electrode-based TENGs, the motion of one layer over the other is considered only in a specific direction for which the results (TENG output power) highly depend on the path of the motions [8-14]. The latter limits the applications of the device in random environmental motions with variable direction.

Researchers have used a capacitive model with two electrodes [11, 15]. The device's performance forced the designer to compensate for the parasitic effect of the inductance. However, the device performance can also be affected by other properties, such as the inductance of the digital electrode arrays [16].

One of the most important shortcomings of the single-electrode-based TENGs is their limitation to a specific sliding direction [8-14]. Therefore, this study proposed a new structure that can convert unpredictable and random movements into electrical power. A sliding TENG with a zero inductance spiral electrode is designed, fabricated, and studied. The device's application for variable directional motions is improved by using a non-directional circular electrode. To examine the possibility of increasing the output power, characterization of the device is done by considering the effect of increasing the number of paralleled devices and increasing the number of spiral turns. Also, the device's performance as velocity and position sensors is studied. Finally, an effective capacitance model is proposed and validated for a single electrode device.

Received: June 2021, Accepted: February 2022

Correspondence to: Dr Tahereh Fanaei Sheikholeslami
Department of Mechanical Engineering,
University of Sistan and Baluchestan, Zahedan, Iran
E-mail: Tahere.fanaei@ece.usb.ac.ir

doi:10.5937/fme2201294H

© Faculty of Mechanical Engineering, Belgrade. All rights reserved

FME Transactions (2022) 50, 294-301 294

2. FABRICATION OF SPIRAL ELECTRODE TENG

A planner spiral electrode TENG was designed, fabricated, and characterized, as shown in Fig. 1. Fig. 1a shows the different layers of the spiral TENG. In this structure, the helical electrode was etched on a copper-coated phenolic board with a thickness of 1.6 mm. Then a polyvinyl chloride (PVC) layer with a thickness of 0.2 mm was placed over it, forming the fixed part of the nanogenerator. PVC and PU are slightly different in electron affinity based on the triboelectric series table.

The fixed part of TENG is scanned by a movable 2 mm polyurethane (PU) layer with a constant frequency of 2 Hz. This part simulates the moving part of the environmental energy source. For example, a PU back-covered mouse slides on a fixed PVC plate or the belt of a manual treadmill when sliding on the fixed shafts. Moreover, the device can be employed as a self-powered real-time sensor to detect omnidirectional sliding motions.

Four samples were fabricated with similar structures but with different turn numbers of 4, 8, 16, and 20. Therefore, the effect of increasing the output power by increasing the device areas and the turn numbers will be studied.

Fig. 1b shows the fabricated spiral electrode on the phenolic board made by chemical etching. The thickness, width, and distance between the electrodes are about 0.035 mm, 0.25 mm, and 1.5 mm. These values are the same for all the fabricated samples. A PVC layer is placed between PU and the spiral electrode to protect the electrode from abrasion. The copper electrode has the role of transferring the induced charges to the output circuit. Here, PU and PVC layers are the triboelectric materials responsible for charge exchanging.

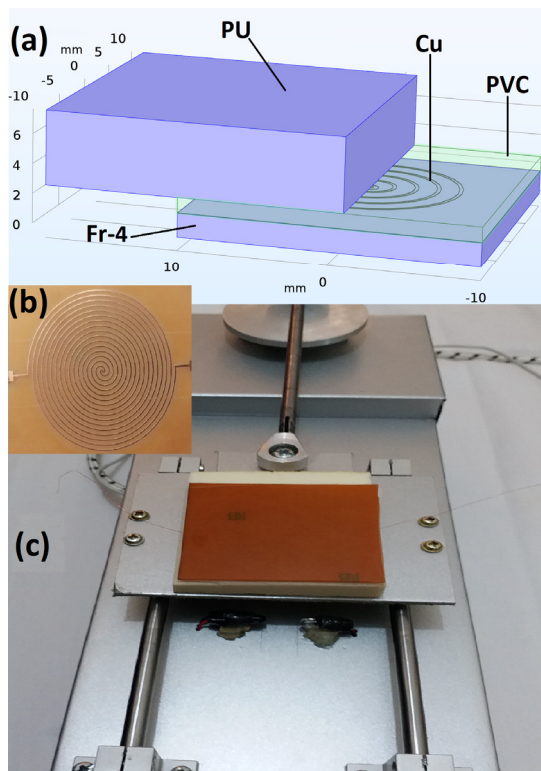


Figure 1. (a) Schematic of the planner spiral TENG; (b) spiral electrode; (c) fabricated instrument for applying mechanical sliding motion.

3. POWER GENERATION MECHANISM

To apply the sliding mechanical force with the desired frequency, and environmental sliding motion simulator was fabricated, as seen in Fig. 1c. This simulator enables us to study the performance of the nanogenerators under different conditions, similar to the environment's mechanical motions. The output current and voltage of all the fabricated TENG samples were measured with a GDM8261 multimeter on a 100 k Ω external load.

The basic mechanism of the power generation by the spiral TENG is believed to be due to the presented triboelectric couple surfaces as PU/PVC, PVC/Fr-4 (Epoxy), and PVC/Cu. The main part of the triboelectric charges is produced by PU/PVC sliding layer because the relative movement of the two other triboelectric couples is very small. However, the direction of the produced currents due to PVC/Fr-4 and PVC/Cu triboelectric couples are by the produced current by the first couple. The latter is because of the electro-negativity order of the materials where the relation is PVC > Cu > Epoxy > PU, based on the triboelectric series table.

The mechanism of electricity generation by the spiral TENG, in various situations of charge distribution for a forward and backward sliding, is schematically shown in Fig. 2. The produced charges between the intermediate layers are not included in the figure. The triboelectric charges generated due to the friction between the two dielectric surfaces will be induced into the metallic electrode. The surfaces of PU and PVC are considered originally slid together in a full overlap position. The transferred triboelectric charges on the surface of PU and PVC can be preserved for a long time due to the nature of the insulator. Once the top PU layer with the positively charged surface starts to slide forward, it will cause a decrease in the induced negative charges on the metallic electrode. Thus the electrons will flow toward the positive parts of the electrode, producing a current signal at its output. When the top PU fully slides out of the PVC layer, the two triboelectric charged surfaces are separated. Therefore, an equilibrium state will occur with no output current. When the PU layer is sliding backward, the induced negative charges on the electrode will increase and thus drive the electrons to flow again and produce a current signal in the opposite direction through the load. When the charged surfaces fully contact again, there won't be any induced charges on the electrode, and the output current will again go to zero.

It should be noted that a spiral electrode, due to its inductance property, negatively affects the produced current and the final generated power of the nanogenerator. This inductance does not contribute to the generating of the triboelectric charges. Still, it can affect the output values of TENG, as an inductive charge transfer element toward the external load. For the proposed spiral structure, where two spiral Archimedean inductors [17] are short connecting at the inner space, the inductance value highly decreases, and the whole element behaves as a resistor. The form of the spiral electrode is presented in Fig. 3. In this figure, D_{out} and D_{in} are the outer and inner diameter, respectively, S

is the interspacing of the electrode arrays, and W is the width of the electrode. A very low inductance of the spiral electrode is one of the advantages of the new design. The low effect of the device inductance will be examined in the result section by changing the number of turns of the spiral electrode.

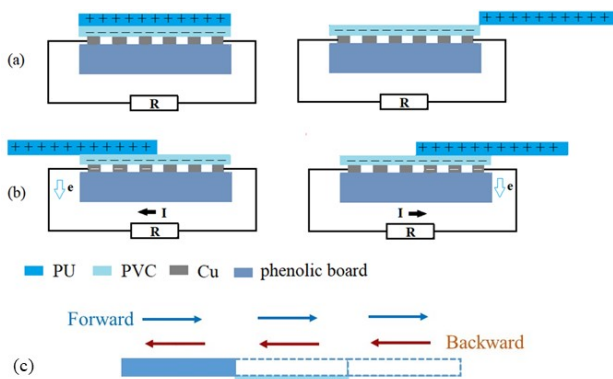


Figure 2. Mechanism of charge distribution and electricity generation by the spiral electrode TENG. a) no-current in full-overlapped and non-overlapped cycles, b) current direction in forward and backward sliding, c) schema for a complete motion.

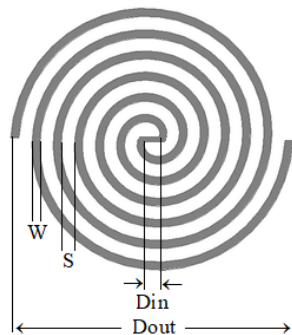


Figure 3. The geometrical form of the proposed spiral electrode for TENG.

4. EXPERIMENTAL RESULTS AND DISCUSSION

4.1 Power Generation Results of TENG

In this section, the results of the experimental measurements for different samples of the spiral electrode TENG are presented and discussed. The output voltage and current of the spiral TENG were measured by applying a 2 Hz alternative sliding force. Therefore, the output current and voltage will be signals with an approximate frequency of 4 Hz. This means two complete forward and reverse sliding motions, resulting in two complete overlaps and two complete nonoverlap in one second (see Fig. 2c).

Fig. 4a and 4b show the samples' measured instantaneous voltage and current with turn numbers of 4, 8, 16, and 20; as the number of spiral turns increases in these figures, the output voltage and current increase from 20 to 100 mV, and from 0.16 to 0.8 μ A, respectively. The increase of the outputs is due to the device's increased area, which leads to increasing the triboelectric produced and transferred charges. Comparing the output voltages and currents for 4 and 20 turns' an approximately five times augmentation is seen, equal to the same ratio between the turn numbers. Similar

relations are observed when comparing the samples with the other number of turns. The average peak-to-peak values for the measured current and voltage are plotted versus the number of turns presented in Fig. 4c, which shows almost a linear curve.

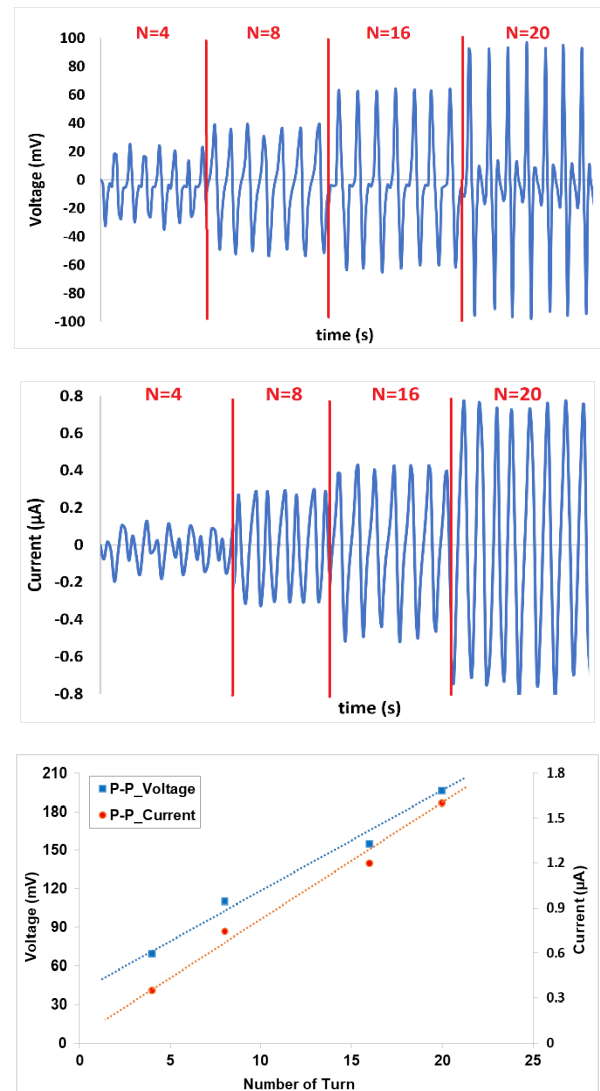


Figure 4. Measured parameters for the spiral electrode TENG with different turn numbers; a) output voltages, b) output currents, c) compared values for output voltages and currents vs. several turns.

Based on the property of an inductive element, the output current decreases when the turn number increases. In Fig. 4c, it is seen that the output current and voltage are almost linearly increased when the turn number of the device is augmented. The higher output power is due to the higher triboelectric area, which leads to the higher value of the produced and transferred triboelectric charges. The latter proves the possibility of ignoring the inductance of the proposed spiral form of the electrode.

It should be noted that the improvement of the device's output using a higher turns electrode is equivalent to the use of a series array of the lower turns electrodes, with a low increase in the area of the device. A parameter for the ratio of the area (AR) is considered for the device. AR is defined as the ratio of the substrate area incorporated with the electrode to the whole area of

the device. By this consideration, AR parameter for the series arrays of the devices would be very close to 1. To investigate the effect of using a parallel array of the device to increase the output power density, the samples fabricated with 4 turns are used. The parallel form is shown in Fig. 5. The measurement results are plotted in Fig. 6. According to Fig. 6a, as the number of the parallel devices increases, at the first step, the output voltage augments and then decreases, for the case with three parallel structures. The voltage increases again for the case with four parallel structures. The behavior is the opposite for the measured current (Fig. 6b). To better show the device behavior, the average peak to peak values for measured currents and voltages are compared in Fig. 6c.

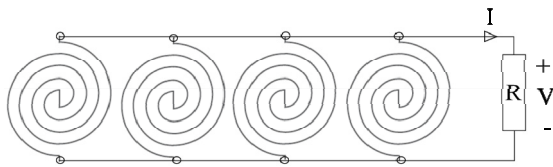


Figure 5. 4-turn spiral TENG in parallel arrays.

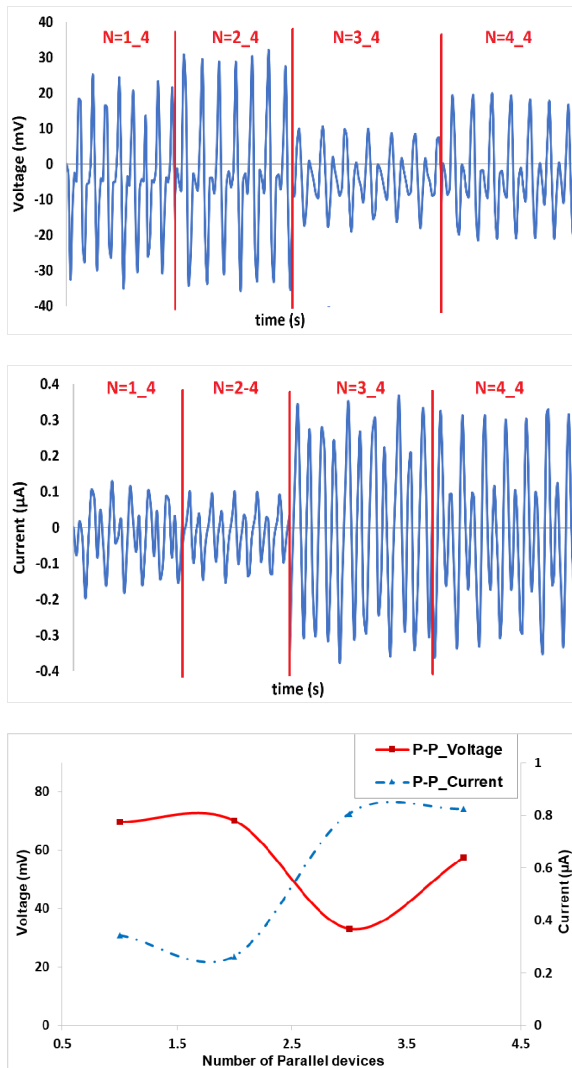


Figure 6. Measured parameters for the structures with different numbers of parallel, a) output voltages, b) output currents, c) compared values for output voltages and currents vs. several parallel devices.

Table 1. Summary of the measurement and calculation results for the fabricated TENG samples with different turn numbers and different numbers of parallel devices.

Turn No.	A (cm ²)	I _m (µA)	V _m (mV)	Avg_Power (nW)
4	1.77	0.34	69.7	1.53
8	15.9	0.74	117.65	6.8
16	28.3	1.08	139.5	10.63
20	44.2	1.61	196.43	20.72
2-4	3.53	0.26	70.2	1.82
3-4	5.3	0.8	33.16	2.84
4-4	7.07	0.82	57.55	3

4.2 Application of TENG as Dynamic Sensors

The TENG devices were characterized based on pre-defined and specific movements. However, the proposed structure can also convert unpredictable and random movements into electrical power. An example is vibrations of the base of machining instruments which result in failures in the final pieces. Therefore, determining the amount of these vibrations is particularly important [18]. The proposed spiral TENG device can be used as a zero power sensor for dynamic measurement of such vibrations and determining the vibration's position in various directions, even for vertical vibrations.

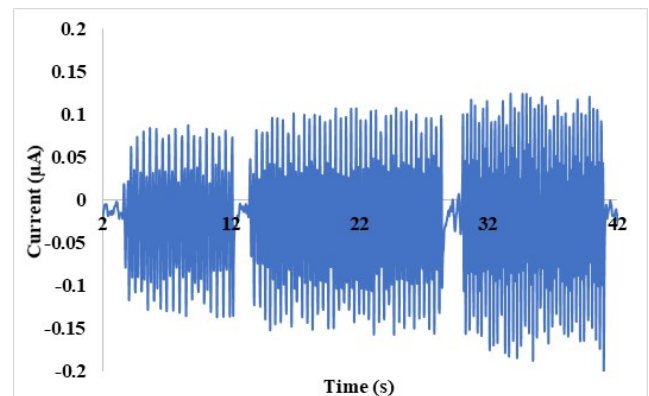
For example, we are placing the device in the table base of a lathe machining instrument to measure the unordered vibrations dynamically.

The performance of the spiral electrode TENG device as velocity and position sensors is examined and presented as follows.

4.3 Velocity Sensor

The designed TENG is used to detect the velocity of a periodic motion without any power supply, which shows an important application of the device as a dynamic zero power velocity sensor.

Fig. 7 shows the output current of an 8-turns and 16-turns spiral electrode device using different frequencies' sliding motions. The device's performance is studied by applying the sliding motions at various speeds. The actual velocities are related to the applied frequencies of 1, 2, and 3 Hz, considering the scanning length of each device (Δx). The total value of Δx , which produces a full-cycle signal, is equal to 13.5 and 18 cm, for 8 and 16 turn devices, respectively.



(a)

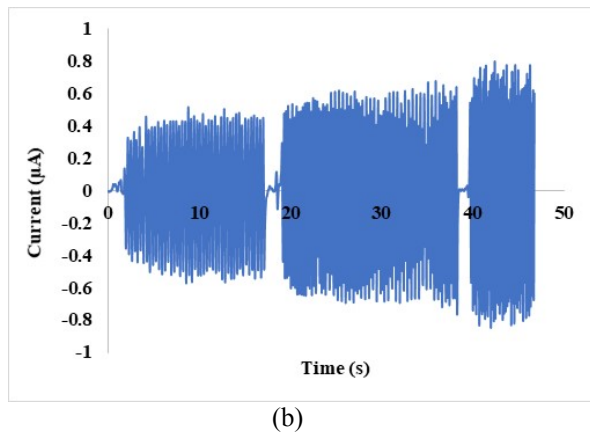


Figure 7. The output current of the spiral electrode device when the sliding motions with three different frequencies are applied on a) 8-turns and b) 16-turns spiral electrode devices.

The results approximately show a linear augmentation in the amplitude of the output current when the velocity of the motion is increased.

The sensor's sensitivity was calculated and plotted using the measured output currents in Fig. 8. In this figure, it is seen that the sensitivity of the proposed velocity sensor is enhanced by increasing the number of spiral turns.

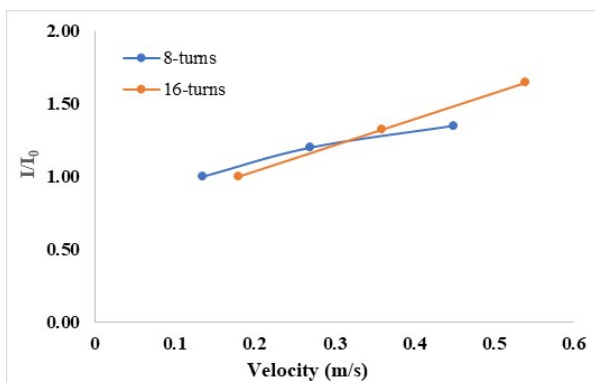


Figure 8. The sensor sensitivity for devices with 8 and 16 turns.

4.4 Position Sensor

The fabricated device is used as a zero power dynamic sensor for detecting the position of a moving object or other physical sources that can apply pressure on a surface.

The proposed device has a circular form such that the spiral arcs are digitally increased from the circle perimeter to the center of the circle. So, it is possible to use the device to detect an object's position when it is moved from the outer circles toward the inner circles. Such a sensor can be applied in the Fabrication of intelligent screens, robotics for automatically adjusting an object position, and other similar situations.

To test the device and show its performance as a position sensor, three relative positions (r_0/r) of 1, 2, and 3 were considered on the 16-turn spiral electrode device, as shown in Fig. 9. The width of each part is 1 cm, where the radius of a 16-turn device (r_0) is 3 cm.

The existence of an object in a specified position (r) was simulated by vertically pressing PU layer over PVC layer with a force of 20 N. The test was repeated 10 times in each position. Simultaneously, the output currents were recorded, which is presented in Fig. 10.

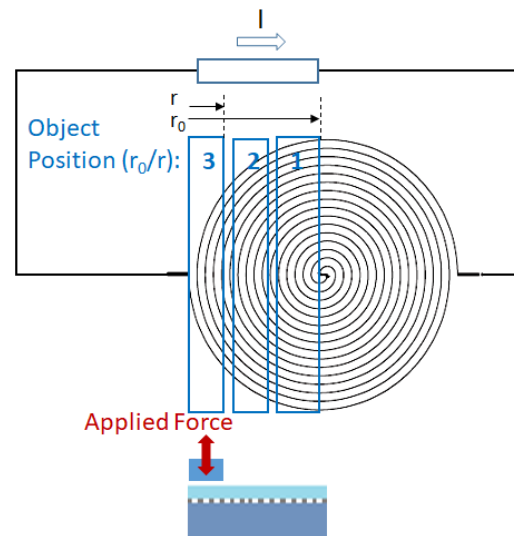


Figure 9. Schema of the characterization method for the location detecting sensor based on a 16-turns spiral TENG.

As seen in Fig. 10, by changing the object's position toward the center of the device, the peak to peak output current is averagely increased from 0.5 to 1 and then to 1.4 μA . The sensor's sensitivity is calculated and plotted vs. relative position in Fig. 11. It is seen that the sensitivity of the sensor is linearly increased when the object gets closer to the center of the circle. The considered positions can be increased by decreasing the width of the force applicator, which is connected to the PU layer.

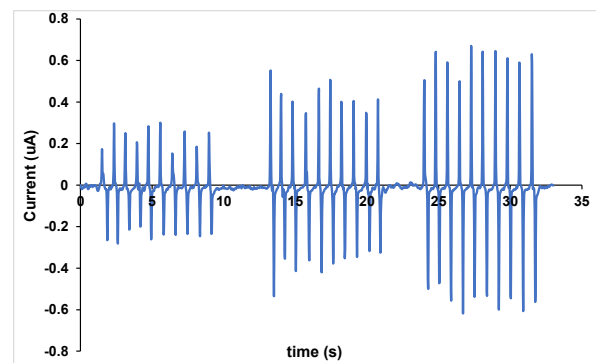


Figure 10. The output current of the position sensor

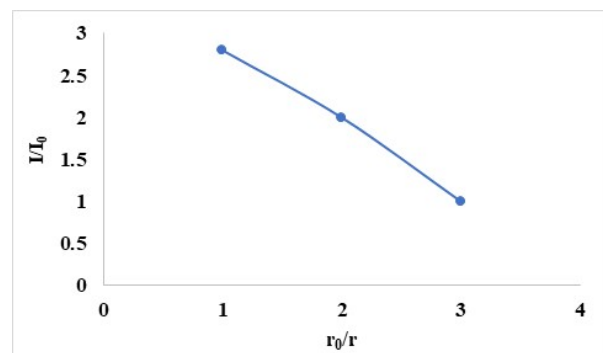


Figure 11. Sensitivity curve of TENG device as a position sensor.

5. CAPACITANCE MODELING OF TENG DEVICE

The behavior of the single spiral electrode TENG is similar to an effective capacitance with the ground of the circuit as the virtual electrode [19-20]. In this section, the spiral electrode TENG is modeled by a triboelectric charge voltage source and an effective capacitance, as presented in the circuit model in Fig. 12. For completing the model, an inductance is considered in the output current path, in addition to the external load resistance, for similar cases with considerable inductance values. But as discussed, the inductance of the designed TENG is too low and can be ignored.

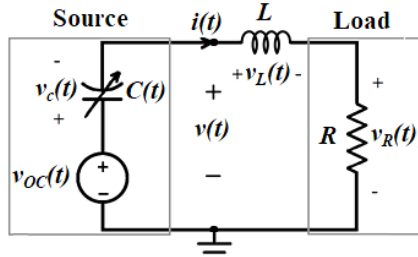


Figure 12. Complete equivalent circuit model for a spiral electrode TENG.

Based on the considered model, a trend is proposed for the length variable capacitor (and therefore a time variable capacitor), schematically presented in Fig. 13. The capacitance value for the device's overlapped region is at the lowest value (zero in the figure), at the starting point ($x=0$), and increases when the movable dielectric, PU, starts overlapping with the fixed PVC layer. When the PU layer is in the middle of the device ($x=l/2$), $C(x)$ reaches its maximum value. Further, when the triboelectric layers are fully overlapped ($x=l$), the effective capacitance is reduced to zero again. At this moment, the direction of motion is changed, and the same behavior is repeated. The capacitor value will again reach its maximum value in full overlapping in the backward motion. Thus, two maximum peaks should be observed for $C(x)$ in a complete reciprocating motion.

In further investigations, the position parameter of x will be converted to the time parameter of t by considering a constant frequency for the sliding motion on the device with the length of l . Equivalent capacitance $C(x)$ will be presented as $C(t)$ in such cases.

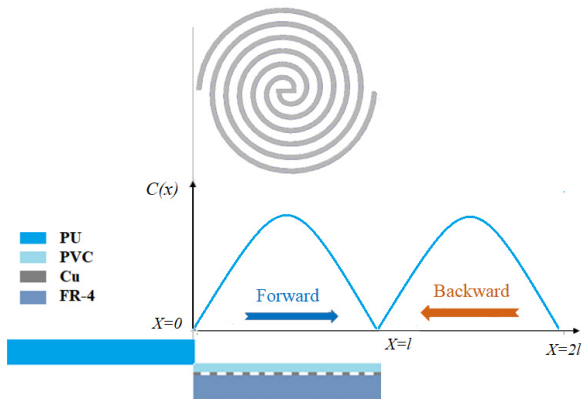


Figure 13. The trend of the equivalent capacitance variations, when the upper movable dielectric, PU, is forward-moving, from $x=0$ to $x=l$.

In order to verify the proposed trend for the capacitive behavior of the device, when it is subject to forward and backward sliding motion, as suggested in Fig. 14, a backward calculation method was used to calculate the effective $C(t)$ based on the experimental results. The calculation procedure is presented as follows.

Considering the circuit equivalent model for the spiral TENG (Fig. 12), the open-circuit voltage is related to the transmitted charges, the area of sliding dielectric surfaces, and the equivalent capacitance of the device as follows:

$$v_{oc}(t) = \frac{\sigma S}{C(t)} \quad (11)$$

where σ is the surface charge density and S is the area of the device. Also, the voltage of the virtual capacitor will be related to the output current as follows:

$$v_c(t) = \frac{1}{C(t)} \int i(t) dt + v_c(0) \quad (12)$$

where $i(t)$ is the measured instantaneous current and $v_c(0)$ is the initial value at $t = 0$. Then, the measured instantaneous voltage corresponds to the following parameters:

$$v(t) = -v_c(t) + v_{oc}(t) \quad (13)$$

By substituting Eqs. 11 and 12 into Eq. 13, the equivalent capacitance value is calculated numerically using the experimental data as follows:

$$C(t_n) = \frac{\sigma(\pi r^2) - \left(\frac{i_{n+1} + i_n}{2} \right) (t_{n+1} - t_n)}{V(t_n) + V(t_n - 1)} \quad (14)$$

where $r=l/2$.

The variations of the calculated effective capacitance of the spiral TENG with 4, 8, and 16 turns' number in two reciprocal sliding motion (in $t = 0.5s$ where $f=2 Hz$) is plotted in Fig. 11. The full overlap in backward and forward sliding occurs at approximately 0.1s to 0.13s ($x=l$) and 0.2 to 0.23s ($x=2l$), respectively, where the capacitance goes to its lowest value for all the samples.

The results confirm the validity of the proposed trend for the capacitive behavior of the single spiral electrode TENG. Because of the high speed of the sliding motion, the two peaks in each direction are overlapped, but when the direction of the sliding motion is reversed, the peaks are separated from the previous peaks.

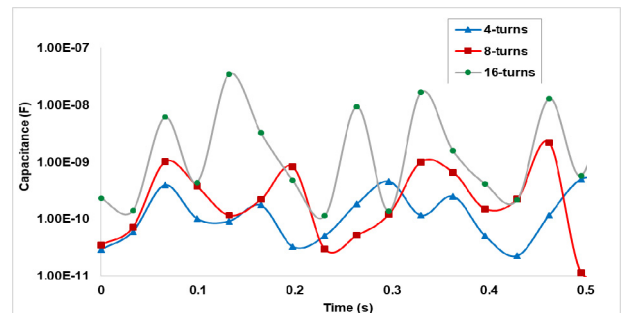


Figure 14. Calculated effective capacitance of the spiral electrode TENG with 4, 8, and 16 turns.

6. CONCLUSIONS

A particular sliding triboelectric nanogenerator with a single spiral electrode was designed and fabricated to harvest sliding mechanical energy regardless of its moving direction. The power generation mechanism for producing and transferring the triboelectric charges was discussed. The performance of the designed nanogenerator was discussed based on its electrical parameters. It was indicated and experimentally shown that the inductance of the device, due to the special consideration form for the spiral electrode, is negligible.

The experimental measurements showed that the output power is augmented by increasing the number of turns of the spiral electrode, which is important for higher amplitude sliding motions. The device is designed to be also used as a dynamic zero-powered multi-directional sensor. The experimental characterization indicates linear sensitivity curves when the device was used as velocity and position sensors.

Finally, adopting the basic theory of TENG device to the present single electrode structure, an effective capacitance was suggested and validated using a backward calculation method for the three different spiral TENG samples with the number of turns from 4 to 16.

REFERENCES

- [1] Patil, B.V., and Sakri, M.: Experimental Studies on the Effect of Shunted Electrical Loads on the Performance of a Vibration-Based Electromagnetic Energy Harvester, *FME Transactions*, Vol. 49, No. 1, pp. 163-172, 202.
- [2] Ismaeel, T.A., Aljabair, S., Abdulrazzaq, O.A. and Abood, Y.A.: Energy Recovery of Moving Vehicles Wakes in Highways by Vertical Axis Wind Turbines, *FME Transactions*, Vol. 48, No. 3, pp. 557-565, 2020.
- [3] Zhang R, Olin H.: Material choices for triboelectric nanogenerators: A critical review, *EcoMat*. Vol. 2, pp. 12062, 2020.
- [4] Chiu S.H, Chen G.R, Tsai Y.C.: Flexible microcavity surface triboelectric nanogenerator for harvesting power in different operating modes, *Japanese Journal of Applied Physics*, Vol. 59, S11J01, pp. 1-7, 2020.
- [5] Cheng L, Xu Q, Zheng Y, Jia X, and Qin Y.: A self-improving triboelectric nanogenerator with improved charge density and increased charge accumulation speed, *Nat. Commun.* Vol. 9, pp. 3773, 2018.
- [6] Chen J, Wang J, Xuan W, Dong S, Luo J.: Universal Triboelectric Nanogenerator Simulation Based on Dynamic Finite Element Method Model, *Sensors*, Vol. 20, pp. 4838, 2020.
- [7] He W, Liu W, Chen J. et al.: Boosting output performance of sliding mode triboelectric nanogenerator by charge space-accumulation effect. *Nat Commun.* Vol. 11, pp. 4277, 2020.
- [8] Luo J, and Wang Z.L.: Recent advances in triboelectric nanogenerator based self-charging power system, *Energy Storage Mater.* Vol.23, pp. 617-628, 2019.
- [9] Jiang T, Chen X, Yang K, Han C, Tang W, Wang Z.L.: Theoretical study on rotary-sliding disk triboelectric nanogenerators in contact and non-contact modes, *Nano Res.* Vol.9, pp. 1057–1070, 2016.
- [10] Du X, Li N, Liu Y, Wang J, Yuan Z, Yin Y, Cao R, Zhao S, Wang B, Wang Z.L, and Li.: Ultra-robust triboelectric nanogenerator for harvesting rotary mechanical energy, *Nano Res.* Vol.11, pp. 1157-1164, 2018.
- [11] Niu S, Wang S, Liu Y, Zhou Y.S, Lin L, Hu Y, Pradel K.C and Wang Z.L.: A theoretical study of grating structured triboelectric nanogenerators, *Energy Environ. Sci.* Vol.7, pp. 2339–2349, 2014.
- [12] Zhu G, Zhou Y.S, Bai P, Meng X.S, Jin Q, Chen J, Wang Z.L.: A shape-adaptive thin-film-based approach for 50% high-efficiency energy generation through micro-grating sliding electrification, *Adv. Mater.* Vol.26, pp. 3788-3796, 2014.
- [13] Meng B, Tang W, Too Z.H, Zhang X, Han M, Liu W, Zhang H.: A transparent single-friction-surface triboelectric generator and self-powered touch sensor, *Energy Environ. Sci.* Vol.6, pp. 3235–3240, 2013.
- [14] Yang Y, Zhang H, Chen J, Jin Q, Zhou Y.S, Wen X, and Wang Z.L.: Single-electrode-based sliding triboelectric nanogenerator for self-powered displacement vector sensor system, *ACS Nano* Vol.7, pp. 7342–7351, 2013.
- [15] Niu S, Wang Z.L.: Theoretical systems of triboelectric nanogenerators, *Nano Energy* Vol.14, pp. 161-192, 2015.
- [16] Mousavi S.H, Kouki A. B.: High-SRF VHF/UHF Lumped Elements in LTCC, *IEEE Microwave and Wireless Components Letters*, Vol. 25, pp. 25-27, 2015.
- [17] Aditya K.: Analytical design of Archimedean spiral coils used in inductive power transfer for electric vehicles application, *Electrical Engineering*, Vol. 100, pp. 1819–1826, 2018.
- [18] Blažević, S., Braut, S., Žigulić, R. and Skoblar, A.: Electromechanical Vibrations of the Vertical Lathe Machining Centre Caused by the Fault of the Working Table Rolling Bearing, *FME Transactions*, Vol. 45, No. 3, pp. 374-381, 2017.
- [19] Chen D, Hu X, and Yang W.: Design of a security screening system with a capacitance sensor matrix operating in single-electrode mode, *Meas. Sci. Technol.* Vol. 22, pp. 114026, 2011.
- [20] Zhang H, Yao L, Quan L, and Zheng X.: Theories for triboelectric nanogenerators: A comprehensive review, *Nanotechnology Reviews*. Vol. 9, pp. 610–625, 2020.

**ДИЗАЈН И ИЗРАДА ТРИБОЕЛЕКТРИЧНОГ
НАНОГЕНЕРАТОРА СА СПИРАЛНОМ
ЕЛЕКТРОДОМ И ПРИМЕНА КАО
ДИНАМИЧКИ СЕНЗОР НУЛТЕ ЧАЏЕ**

**М.А. Хејдари, Т.Ф. Шенкхолеслами,
А. Бехзадмер**

Сакупљање енергије из кретања околине је ефикасан метод за припрему трајних извора напајања за интелигентне бежичне системе. У овом раду је произведен и истражен трибоелектрични наногенератор са једном спиралном електродом (ТЕНГ) за прикупљање енергије из вишесмерних клизних покрета. Уређај је предвиђен да се користи и као сензор динамичке брзине са сопственим напајањем. У првом кораку, четири узорка се израђују и карак-

теришу применом клизних покрета од 2 Хз. Резултати показују повећање излазне снаге са 1,53 на 20,72 нВ, за уређај са 4 до 20 обртаја. Да би се упоредили резултати, такође се проучава ефекат повећања излазне снаге коришћењем паралелног низа. У следећем кораку истражује се примена уређаја као сензора брзине и положаја. Линеарна зависност између улаза и излаза сензора примећује се код уређаја са 8 и 16 спиралних завоја. На крају, представљено је моделирање кола за уређај и предложен је тренд за виртуелно капацитивно понашање једне електроде ТЕНГ.